

Nonlinear Forced Response Synthesis with Quasi-Static Modal Analysis

Robert J. Kuether

Senior Member of Technical Staff, Sandia National Laboratories¹, Albuquerque, NM, USA 87185

David A. Najera

Project Engineer II, ATA Engineering Inc., San Diego, CA, USA 92128

ABSTRACT

Recent computational developments have been made to approximate the amplitude dependent modal properties of assembled structures with frictional interfaces using quasi-static modal analysis. These methods were initially applied to reduced order models with discrete Iwan elements to capture joint nonlinearity and have been extended to large-scale finite element models with Coulomb friction and contact. The predicted nonlinear natural frequencies and damping ratios provide valuable insights into the behavior of jointed structures, particularly the level of modal damping due to frictional losses and microslip. This work develops an algorithm that utilizes the results from quasi-static modal analysis to quickly compute the nonlinear forced response for the structure. The approach assumes a single nonlinear resonant mode with amplitude dependent natural frequencies and damping ratios, and accounts for the off-resonant terms with linear mode solutions. A comparison to direct time integrated solutions demonstrates the accuracy of the approach to efficiently obtain harmonically forced, steady-state solutions of nonlinear finite element models.

Keywords: *nonlinear forced response, quasi-static modal analysis, frictional energy dissipation, nonlinear resonant mode, nonlinear damping*

1. Introduction

Bolted joints and other joining technologies in mechanical engineering designs introduce several challenges to adequately model and predict the appropriate stiffness and energy dissipation of assembled, load-bearing structures. The presence of frictional contact in mechanical interfaces contribute to this challenge due to the small length scales required to model the physics. Several researchers have explored methods to model damping in mechanical systems due to joints, for example see review papers [1, 2]. As observed both experimentally and numerically, the presence of joint damping introduces energy dissipation that depends on response amplitude, causing the resonant peaks of the normalized forced response curves to decrease. Localized frictional slip, or microslip, is responsible for the increase in damping at larger response levels of the resonant mode. In addition to the nonlinear damping, the resonant frequency slightly decreases due to loss of stiffness in the joint when low-pressure regions of the joint begin to slip. The resonant mode causes the peak to change in these ways depending on how much the mode shape under consideration loads the joints in the system.

¹ Sandia National Laboratories is a multimission laboratory managed and operated by National Technology & Engineering Solutions of Sandia, LLC, a wholly owned subsidiary of Honeywell International Inc., for the U.S. Department of Energy's National Nuclear Security Administration under contract DE-NA0003525.

The frequency response function (FRF) for linear systems provides the amplitude *independent* relationship between the input force and output response of the system. The FRF is calculated in the frequency domain either directly from the system matrices or as a synthesis of a truncated modal solutions (i.e. linear superposition). In the presence of nonlinearity, alternate solution methods are needed to compute the nonlinear forced response (NLFR) curves at each forcing amplitude of interest. One approach is the direct time integration method applied to the nonlinear system of ordinary differential equations to obtain steady-state solutions for each forcing frequency. This approach is time consuming and only applicable to low order models with sufficient damping. In addition, time integration methods have the potential to neglect key nonlinear solutions and features in the response curves (i.e. multiple stable solutions, isolas, etc.). The multi-harmonic balance method combined with path-following techniques is another common approach to obtain the NLFR for models with frictional contact [3]. The approach is more efficient compared to direct time integration since it solves nonlinear algebraic equations in the frequency domain for each forcing frequency and amplitude. The method requires specialized codes that are not readily available within commercial finite element packages and hence make it difficult to solve large-scale, high fidelity models without significant investment in code development.

This research presents an approach to synthesize the nonlinear forced response curves using the nonlinear resonant mode approximation developed by Szemplinska-Stupnicka [4] and later refined by Krack et al. [5]. The approach treats the modal transfer function in the frequency domain as a nonlinear algebraic equation such that the mode shape, frequency and damping ratio are nonlinearly dependent on energy or response amplitude. Krack et al. utilized the complex nonlinear normal mode approach by Laxalde et al. [6] to obtain the nonlinear modal properties within the NLFR framework. This approach is adapted in this research to specifically address structures with mechanical interfaces by using the quasi-static modal analysis (QSMA) approach to obtain the amplitude dependent resonant frequency and damping ratio of a finite element model. The QSMA approach originally developed by Festjens et al. in [7] was later extended by Lacayo et al. [8] to reduced order models with four-parameter Iwan elements. The technique was further developed to non-intrusively obtain nonlinear modal data from large-scale finite element models created using commercial software packages [9]. The method is applied through the development of wrapper algorithms that either sends or receives the inputs and outputs from the nonlinear static solver. QSMA obtains the backbone data to describe how a specific resonant mode is affected by the joints in the system by approximating the change in damping ratio, sometimes orders of magnitude, and shift in resonant frequency due to joint slipping.

The remainder of the paper is organized as follows. Section 2 provides the theoretical overview of the NLFR synthesis using the nonlinear resonant mode approximation. The section describes the solution technique for the nonlinear algebraic equation and the QSMA algorithm developed for finite element models with four-parameter Iwan elements. The approach is demonstrated in Section 3 on a C-Beam bolted assembly model with two Iwan elements to capture microslip due to shear loading in the joint. The QSMA results are obtained and used to predict nonlinear forced response curves at various force amplitudes. The results are compared with direct time integrated steady-state solutions to evaluate the accuracy of the approximation and better understand the cost savings of the technique. The conclusions and future directions of the research are presented in Section 4.

2. Theoretical Development

The steady-state response for a linear, second order system of equations is calculated by transforming the model response from the time domain into the frequency domain. A harmonic input force assumes the mathematical form,

$$\mathbf{f}_{ext}(t) = \text{Re}\{\mathbf{F}e^{i\omega t}\} \quad (1)$$

where \mathbf{F} is the $N \times 1$ complex vector of the applied force, ω is the angular frequency of the oscillatory force, and t is time. Following the derivation of the harmonic response of a linear system with light viscous damping, and decomposing the response into modal contributions [10], the modal transfer function from input force, \mathbf{F} , to the complex modal response amplitude, $Q_k(\omega)$, is,

$$Q_k(\omega) = \frac{\Phi_k^T \mathbf{F}}{-\omega^2 + \omega_k^2 + 2i\zeta_k \omega_k \omega} \quad (2)$$

In this equation, Φ_k , ω_k , and ζ_k are the $N \times 1$ mass normalized real eigenvector, natural frequency, and modal damping ratio for the k^{th} mode, respectively. Solving for the complex modal amplitude at each input frequency provides the modal scaling for the k^{th} mode shape. Each modal contribution in the physical domain becomes,

$$\mathbf{X}_k(\omega) = \Phi_k Q_k(\omega) \quad (3)$$

where $\mathbf{X}_k(\omega)$ is the $N \times 1$ complex vector of the physical response at all degrees-of-freedom (DOF). Summing all the physical responses from each modal contribution results in the linear superposition of modal responses in the frequency domain, where m is the total number of modes used in the reconstruction,

$$\mathbf{X}(\omega) = \sum_{k=1}^m \mathbf{X}_k(\omega) = \sum_{k=1}^m \Phi_k Q_k(\omega) \quad (4)$$

The $N \times 1$ complex vector, $\mathbf{X}(\omega)$, accounts for all contributions of the modal response in the physical space and is a well-suited approximation of the transfer function for a linear system. The frequency domain transfer function in Eq. (4) is transformed back to the time domain as,

$$\mathbf{x}(t) = \text{Re}\{\sum_{k=1}^m \mathbf{X}_k(\omega) e^{i\omega t}\} = \text{Re}\{\sum_{k=1}^m \Phi_k Q_k(\omega) e^{i\omega t}\} \quad (5)$$

A modal approach to calculate the steady-state forced response has the advantage of quickly evaluating Eq. (2), which is a one-dimensional complex equation, over the entire frequency band of interest. Alternative direct calculations of the transfer function require inversion of $N \times N$ system matrices for each forcing frequency and is a less efficient operation to obtain the solution in Eqns. (4) and (5), albeit there is no approximation in the direct approach. The modal approach does require the calculation of the real modes using an appropriate eigen solver. The following subsections adapt this linear modal decomposition of the transfer function to weakly nonlinear structures with frictional contact at jointed interfaces.

2.1 Nonlinear Resonant Mode Approximation

All developments thus far have assumed a linear system and thus are perfectly valid approximations for synthesizing the response as a linear superposition of mode solutions. Modal truncation error is well-understood for these techniques and can be mitigated by including sufficient modes with frequencies in the range of the harmonic forcing, or by including residual terms. This work extends this approach to weakly nonlinear systems by simply using amplitude dependent natural frequencies and damping ratios calculated from the QSMA algorithm. The nonlinear extension uses the single-resonant mode approximation originally proposed by Szemplinska-Stupnicka [4], which assumes that the nonlinearity is weak such that the coupling terms of the modal coordinates are negligible, and the modes are well-spaced in frequency. These assumptions allow a single resonant mode to be treated as nonlinear such that the modal transfer function in Eq. (2) can be modified as,

$$Q_r(\omega, Q_r) = \frac{\Phi_r^T \mathbf{F}}{-\omega^2 + \omega_r^2(|Q_r|) + 2i\zeta_r(|Q_r|)\omega_r(|Q_r|)\omega} \quad (6)$$

The amplitude dependent natural frequency, $\omega_r(|Q_r|)$, and damping ratio, $\zeta_r(|Q_r|)$, explicitly depend on the magnitude of the complex modal response amplitude. The nonlinear equation in Eq. (6) must be solved iteratively to calculate the resonant mode response at frequencies near the r^{th} resonant mode of interest. For jointed structures, the modal parameters are computed directly by solving a series of quasi-static responses to an externally applied modal force. For QSMA and the approximate nonlinear transfer function in Eq. (6), it is assumed that the mode shapes do not change as the response amplitude changes. The evolution of the damping ratio and natural frequency occur due to frictional losses in the jointed interfaces as the deflection into the mode shape imparts loads on the joint. Typically, this results in a loss of stiffness for the vibration mode but increase in energy dissipation due to localized frictional slip, i.e. microslip.

As proposed by Krack et al. [5], the response of the system in the physical domain can be synthesized by appending the solution from the nonlinear resonant mode with the linear, non-resonant modes,

$$\mathbf{X}(\omega) = \Phi_r Q_r(\omega, Q_r) + \sum_{k \neq r}^m \Phi_k Q_k(\omega) \quad (7)$$

The additional linear terms account for the modal contributions that are assumed to be excited at low amplitudes due to the assumption of well-spaced modes. The time domain approximation to the harmonic response can be obtained similarly using Eq. (5). The advantage of this approach is that the responses can still be decomposed into one-dimensional complex equations, only now that the resonant mode is nonlinear and requires the use of iterative solvers.

2.2 Solving the Nonlinear Resonant-Mode Equation

The nonlinear resonant mode transfer function in Eq. (6) requires an iterative technique to obtain solutions for the modal amplitude, Q_r , for a set of input frequencies, ω , due to the dependence of amplitude in the natural frequency and damping ratio. This solution is obtained using a Newton-Raphson algorithm to find the root of a real-valued residual equation. The approach starts by rearranging Eq. (6) into a residual equation of the form,

$$R^*(\omega, Q_r) = (-\omega^2 + \omega_r^2(|Q_r|)) + 2i\zeta_r(|Q_r|)\omega_r(|Q_r|)\omega)Q_r - \Phi_r^T \mathbf{F} \quad (8)$$

where R^* is a complex scalar value. This residual equation is explicitly written in terms of the real and imaginary parts to provide a real-valued equation,

$$\mathbf{R}(\omega, Q_r) = \begin{Bmatrix} R^r \\ R^i \end{Bmatrix} = \begin{Bmatrix} -\omega^2 Q_r^r - 2\zeta_r(|Q_r|)\omega_r(|Q_r|)\omega Q_r^i + \omega_r^2(|Q_r|)Q_r^r - \Phi_r^T \mathbf{F} \\ -\omega^2 Q_r^i + 2\zeta_r(|Q_r|)\omega_r(|Q_r|)\omega Q_r^r + \omega_r^2(|Q_r|)Q_r^i \end{Bmatrix} \quad (9)$$

where $Q_r = Q_r^r + iQ_r^i$ is the complex modal amplitude in terms of real and imaginary parts.

The real-valued residual equation in Eq. (9) is a 2×1 nonlinear algebraic equation that is solved with a damped Newton-Raphson iterative scheme to minimize the L2 norm of the residual equation. The damped Newton-Raphson algorithm successively updates the solution to provide a better approximation to the root as,

$$Q_{r,n+1} = Q_{r,n} - \varepsilon \left[\frac{\partial \mathbf{R}}{\partial Q_r} \right]^{-1} \mathbf{R}(Q_r) \quad (10)$$

where n is the index of the iteration, and ε is the relaxation factors that weighs contribution from the correction term (value between 0 and 1). The solution is iteratively updated until the L² norm of the residual falls below a prescribed numerical tolerance such that,

$$\frac{\|\mathbf{R}(\omega, Q_r)\|}{\|\Phi_r^T \mathbf{F}\|} \leq \delta_{rel} \quad (11)$$

The scalar value δ_{rel} defines the threshold below which the solution is considered converged. Typical values of the relative tolerance are between 1E-6 and 1E-4 depending on the convergence and stability of the problem.

2.3 Nonlinear Modal Characteristics of Jointed Structures

The quasi-static modal analysis algorithm is used to determine the nonlinear natural frequencies and damping ratios of the resonant-modes of interest. The approach is developed to capture the change in frequency due to loss in stiffness in joints as well as increase in energy dissipation due to localized frictional slip. In this research, the joint physics are modeled using the four-parameter Iwan element [11] to capture microslip in a bolted joint. The joint modeling approach is combined with a Hurty/Craig-Bampton (HCB) [12-14] reduced order model to reduce the interior DOF assumed to be linear, while retaining the local attachment nodes to connect the nonlinear constitutive elements. Details of this modeling approach can be found in [15].

The details of the QSMA method are provided in [8] but summarized here for completeness. Starting with the equations-of-motion for the reduced order model with Iwan elements,

$$\mathbf{M}\ddot{\mathbf{x}} + \mathbf{C}\dot{\mathbf{x}} + \mathbf{K}\mathbf{x} + \mathbf{f}_{nl}(\mathbf{x}, \boldsymbol{\theta}) = \mathbf{f}_{ext}(t) \quad (12)$$

where \mathbf{M} , \mathbf{C} , and \mathbf{K} are the $N \times N$ mass, damping and elastic stiffness matrices, respectively. The $N \times 1$ nonlinear force vector contains the contribution of the four-parameter Iwan element to capture frictional slip in the joint regions of the finite element model. The QSMA method applies a force to the quasi-static system of equations

proportional to the shape of the resonant, linear mode of interest. The quasi-static form of the equations is obtained by neglecting the inertia and viscous damping terms in Eq. (12),

$$\mathbf{K}\mathbf{x} + \mathbf{f}_{nl}(\mathbf{x}, \boldsymbol{\theta}) = \mathbf{M}\boldsymbol{\Phi}_r\boldsymbol{\alpha} \quad (13)$$

The modal force on the right-hand side is scaled by α to increase the amount of force input to the model. The force is pre-multiplied by the mass matrix such that at low force levels, the force causes the model to exactly deflect into the r^{th} mode shape due to the orthogonality properties of the system. The modes are calculated about the linearized equilibrium state,

$$\left(\mathbf{K} + \frac{\partial \mathbf{f}_{nl}(\mathbf{x}, \boldsymbol{\theta})}{\partial \mathbf{x}} \Big|_{\mathbf{x}=0} - \omega_r^2 \mathbf{M} \right) \boldsymbol{\Phi}_r = \mathbf{0} \quad (14)$$

Solving Eq. (13) for varying levels of force scaling results in amplitude dependent responses, $\mathbf{x}(\alpha)$. Applying a modal filter to project the response onto the modal coordinates results in the resonant mode amplitude, $q_r(\alpha)$. Following the theory in [8], the amplitude dependent natural frequency is approximated as the secant to the modal backbone curve,

$$\omega_r(q_r) = \sqrt{\alpha/q_r(\alpha)} \quad (15)$$

The amplitude dependent damping ratio is computed as,

$$\zeta_r(q_r) = \frac{D(\alpha)}{2\pi(q_r(\alpha)\omega_r(q_r))^2} + \zeta_{0,r} \quad (16)$$

where $D(\alpha)$ is the energy dissipated per oscillation cycle of the modal hysteresis curve and $\zeta_{0,r}$ is the linear modal damping ratio due to material damping. The results from Eqn. (15) and (16), combined with the linearized mode shape, $\boldsymbol{\Phi}_r$, from Eq. (14) provide the necessary terms to compute the nonlinear resonant modal transfer function in Eq. (6). The linearized, off-resonant modes from Eq. (14) can be used to compute the additional linear terms in Eqns. (2) and (7).

3. Numerical Results: C-Beam Assembly

The NLFR method is demonstrated on the C-Beam assembly which has two, localized bolted connections on each end. The finite element mesh, created in Cubit [16], is shown in the left image in Figure 1. The mesh had a total of 579,092 8-noded reduced integration hexahedral elements, where the total element count was determined based on a convergence study of the modal frequencies. The model had simple supports at two opposite edges of the bottom beam to restrict rigid body motion. The beam material was assigned isotropic linear elastic properties corresponding to 440C stainless steel with a Young's modulus of 29,000 ksi (200 GPa), Poisson's ratio of 0.283, and mass density of 7.123E-04 lbf-s²/in⁴ (7600 kg/m³). A whole joint modeling approach, shown in the right image of Figure 1, was used to approximate the frictional contact interfaces of the bolted connection. The interface nodes assumed to be in contact from a nonlinear preload analysis were condensed down to a single virtual node by multi-point constraints (MPCs). The opposing virtual nodes for the mating surfaces were then connected with one-dimensional constitutive elements to describe the joint forces, totaling six relative DOF per whole joint. A four-parameter Iwan element was used to model the joint forces in the relative X displacement direction with the set of values listed in Table 1. All other whole joint DOF were modeled as linear springs with either 1E+12 lbf/in or 1E+12 lbf-in/rad depending on translational or rotational DOF. As described in the theory section, an HCB reduced order model was created to reduce the linear, interior DOF of the model while maintaining the virtual nodes of the MPCs and input locations as physical, boundary DOF. The HCB model had a total of 25 fixed-interface modes to capture frequencies up to 6,200 Hz. A total of 27 static constraint modes were computed to capture the 24 boundary DOF associated with the whole joint connections (six per surface), and three boundary DOF corresponding to the input node at the center of the top beam.

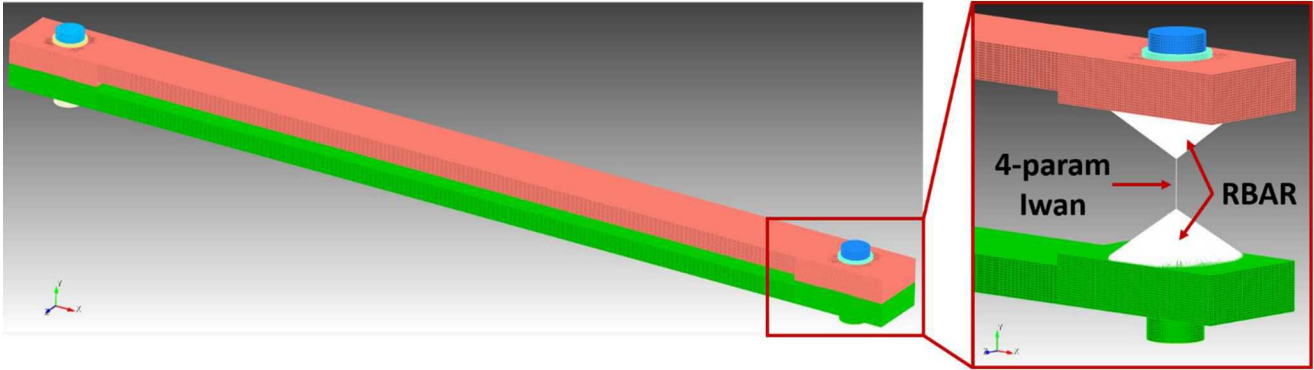


Figure 1. Schematic of C-Beam structure with whole joint model to capture joint nonlinearity.

Table 1. Four-parameter Iwan values in the x-displacement DOF of the whole joint model.

K_T	F_S	χ	β
5.125E+06 lbf/in	1086 lbf	-0.5714	1.783E-03

The first vibration mode of the nonlinear HCB model was selected to demonstrate the NLFR synthesis approach based on QSMA modal data to capture the effect of joint microslip. The first mode shape is shown in Figure 2, which was an in-phase bending mode that applied a relative shear load in the X direction of the joint. The four-parameter Iwan element captures the localized slip in this shear direction for increasing vibration and load levels. The QSMA results for this first mode's nonlinear natural frequency and damping ratio are shown in Figure 3. The left figure plots the nonlinear natural frequency as a function of the modal displacement amplitude, $|q_1|$. The black dashed line corresponds to the linearized natural frequency determined by setting the Iwan element to a linear spring with the tangent stiffness value of $K_T = 5.125E+06$ lbf/in. The right figure shows the nonlinear damping ratio for the first mode where the blue dashed curve corresponds to the nonlinear portion of damping from the frictional slip in the Iwan element; this is the first term in Eq. (16). The nonlinear damping contribution was appended to a baseline linearized viscous damping term to capture the inherent material damping in the structure at low response amplitudes when the joint remains stuck. A linear modal damping ratio of 0.5 % was assumed for the analysis. The QSMA results in Figure 3 converged to the linearized frequency and damping at low response amplitude when little to no slip occurred in the Iwan element. As the amplitude of the modal response increased, the joint began to slip causing the damping ratio to increase and the natural frequency to decrease.



Figure 2. First in-phase bending mode of the linearized beam at 217.4 Hz.

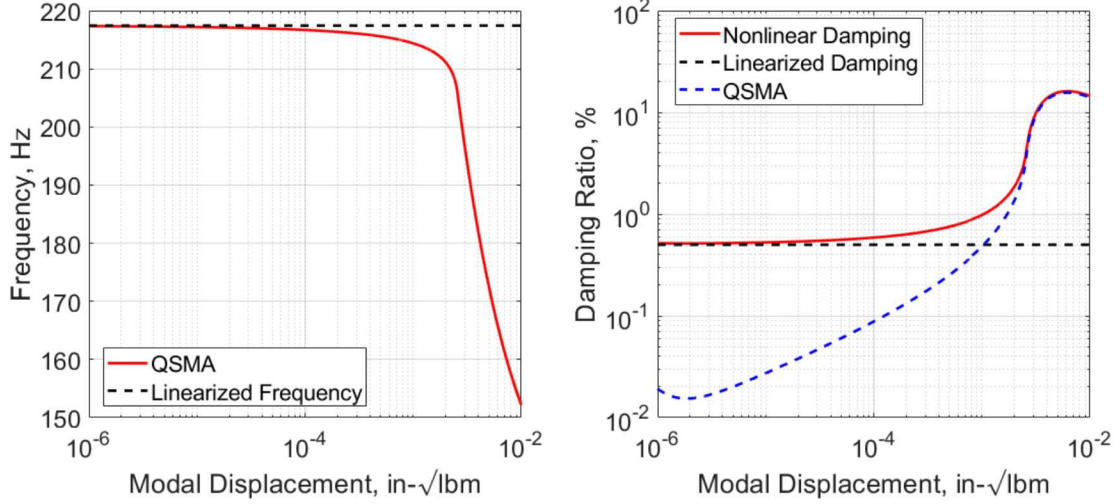


Figure 3. (Left) Nonlinear resonant frequency and (right) nonlinear damping predicted with QSMA.

The results in Figure 3 were used in the NLFR synthesis approach in Eq. (7) to predict the drive-point response at various force amplitudes. The input force was applied in the y-direction at the middle point of the top beam for forces amplitudes ranging from 0.1 lbf and 50 lbf. The input frequencies were applied between 180 and 240 Hz to excite the first resonant in-phase bending mode. The plot in Figure 4 shows the magnitude of the NLFR predicted drive-point displacements (colored lines) in the y-direction for nine different force amplitudes. The results from NLFR synthesis were compared to the steady-state solutions obtained from direct time integration of the harmonically force HCB equations of motion (black dashed). At low forcing amplitudes (0.1 lbf to 0.5 lbf), the response of the beam appeared to be linear as there was no apparent shift in the resonant frequency or change in the general shape of the curve. As the forcing amplitude increased, the peak began to bend to the left and broaden due to the decrease in resonant frequency and increase in the energy dissipation due to joint microslip. The NLFR visually agreed well with the time integrated reference solution for all forces between 0.1 lbf and 10 lbf. Slight discrepancies arose for the highest considered loads of 20 and 50 lbf, which appeared to shift the resonance by approximately 11% and put the joint into a state of macroslip. These load cases would be considered beyond the scope of the modeling approach since the approximate NLFR solution may not capture more complex, strongly nonlinear behavior. These results were shown for completeness to demonstrate the accuracy of the method beyond microslip.

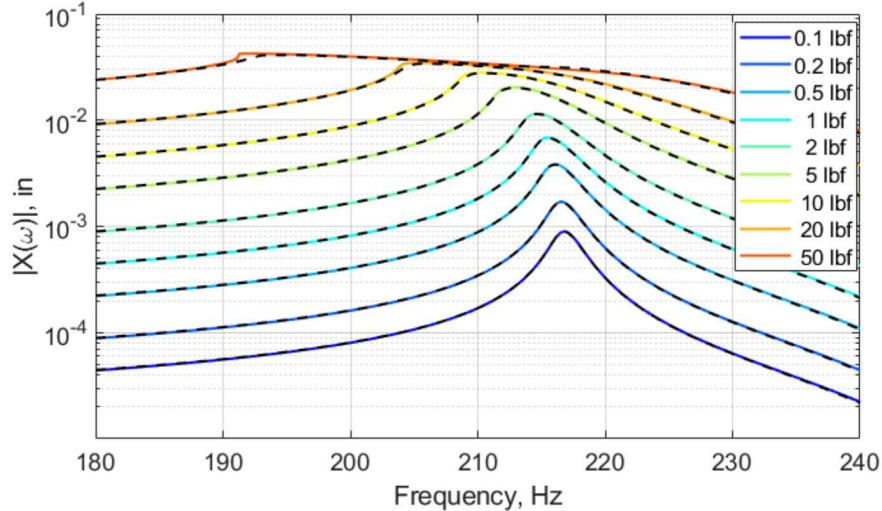


Figure 4. Comparison of nonlinear forced response curves (solid colored lines) with steady-state response amplitudes obtained with direct time integration (black dashed).

In addition to the visual comparison, a quantitative comparison was performed by using a modification to the Frequency Response Assurance Criterion (FRAC) [17] based on the magnitude of the forced response curves. The modified FRAC (mFRAC) in this work is computed as,

$$mFRAC = \frac{\sum_{\omega=\omega_1}^{\omega_2} |X_i|_{NLFR}(\omega) |X_i|_{DT}(\omega)}{\sum_{\omega=\omega_1}^{\omega_2} |X_i|_{NLFR}(\omega) |X_i|_{NLFR}(\omega) \sum_{\omega=\omega_1}^{\omega_2} |X_i|_{DT}(\omega) |X_i|_{DT}(\omega)} \quad (17)$$

where the magnitude of the i^{th} response point is defined as $|X_i|$, and ω_1 and ω_2 are the frequency limits of the solution. The mFRAC metric is bounded between 0 and 1, where a value of 1 corresponds to perfect correlation of the forced response curves predicted with the NLFR algorithm and direct time integration. The mFRAC correlation values for the drive-point response curves in Figure 4 are provided in Table 2 and were computed as 1.0000 for all forced response curves with forcing amplitude between 0.1 lbf and 5 lbf. The largest error was for the 10 lbf case with a value of 0.9991, which still corresponds to an excellent correlation. The correlation metric agrees with the visual comparison, confirming excellent agreement between the approximate NLFR and direct time integration methods.

Table 2. mFRAC of the approximate NLFR and direct time integration methods.

Force Amplitude	0.1 lbf	0.2 lbf	0.5 lbf	1.0 lbf	2.0 lbf
mFRAC	1.0000	1.0000	1.0000	1.0000	1.0000
<hr/>					
Force Amplitude	5.0 lbf	10 lbf	20 lbf	50 lbf	
mFRAC	1.0000	0.9999	0.9991	0.9992	

Regarding the computational cost, the NLFR algorithm took 13.2 seconds on a single processor in Matlab to calculate the forced response at 240 frequency points. The offline cost associated with the QSMA algorithm was only 1.8 seconds on a single processor, totaling 15.0 seconds for combined offline and online cost. The direct time integration method took 17,000 seconds (or 4.7 hours) on a single processor to obtain the same number of solutions from the HCB model with two Iwan elements. A convergence study was performed, and it was determined that the solution needed to be integrated over 250 cycles to reach a converged steady-state solution. The light damping in the system away from the resonance caused transients to contaminate the results without enough time to allow them to decay. The NLFR achieved a 1133x reduction in computational cost for the forced response simulations in comparison to the direct time integrated approach.

The plot in Figure 5 shows the same force response curves as in Figure 4 but now only plots the contribution of the first modal amplitude, $|Q_1|$, as calculated by Eq. (6) (colored curves). The backbone frequency curve from QSMA (black dashed) was overlaid in this figure to demonstrate how the modal forced response resonance peaks follow the backbone of the nonlinear mode. This plot, combined with the QSMA data plot in Figure 3, can be used to interpret the range of applicability for the NLFR algorithm. For example, the power-law damping behavior in Figure 3 between approximately $|Q_1| = 1E-6$ and $2E-3 \text{ in} - \sqrt{\text{lbf}}$ shows that the model was in a state of microslip in these ranges of modal amplitudes. This information combined with the modal forced responses in Figure 5 suggest that the harmonic force started to induce macroslip behavior in the joints above ~ 10 lbf amplitude. This can provide engineers with a useful design tool to understand the load bearing capabilities of the joint under harmonic excitation, and to quantify when significant slip will introduce vibration induced wear in the joints.

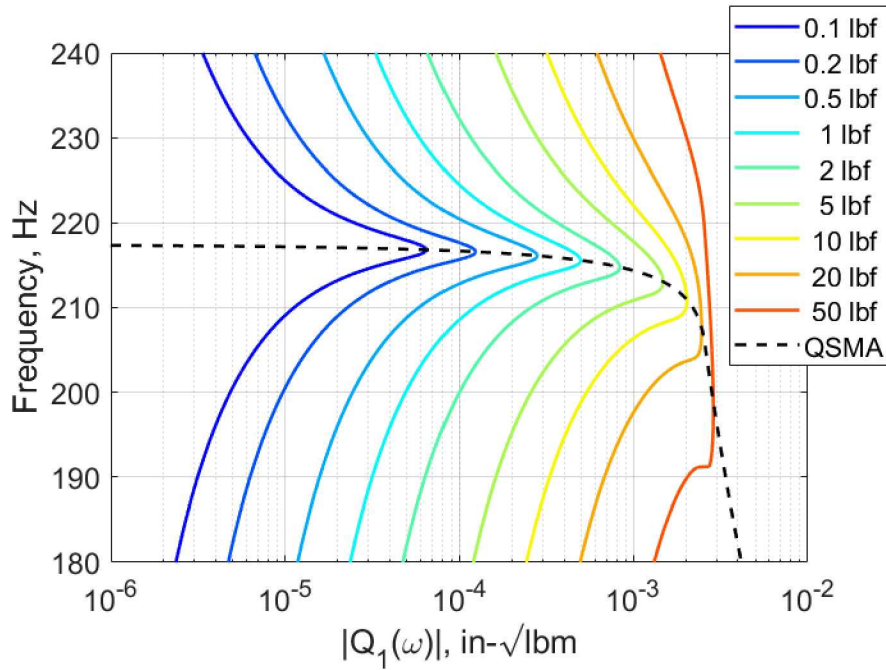


Figure 5. Frequency versus mode one displacement amplitude for various nonlinear force response curves.

4. Conclusion

In this research, the nonlinear forced response algorithm based on the single nonlinear resonant mode assumption was combined with the quasi-static modal analysis approach to efficiently calculate the steady-state forced response to a harmonic excitation. The QSMA algorithm provides an efficient method to approximate the influence of mechanical joints on the modal characteristics of a finite element model by solving a series of quasi-static analyses in addition to a linearized eigenvalue problem. The algorithm has been successfully developed and used for models with four-parameter Iwan elements to capture microslip effects on the dynamic response.

Recently the algorithm has been applied to large-scale finite element models by wrapping the algorithm around a nonlinear static solver in commercially available software, allowing this approach to be extended to detailed finite element models of interest to industry. The new method was demonstrated on a C-Beam assembly with two bolted joints modeled as Iwan element in the shear direction. Comparing the steady-state solutions from direct numerical integration and the NLFR algorithm with QSMA, the modified frequency response assurance criterion confirmed that the approximate NLFR results agrees extremely well with the reference solution with a correlation value of 1.000 for all forcing amplitudes considered. The new algorithm demonstrated a 1133x reduction in computational cost while maintaining a high level of accuracy. This research demonstrates the applicability of QSMA to the NLFR technique for finite element models with weak nonlinearity (i.e. microslip region of bolted joints) and well-separated modal frequencies. The success of the method warrants future work to explore the use of NLFR with QSMA data obtained from high-fidelity finite element models to obtain the steady-state solutions to an arbitrary harmonic excitation.

Acknowledgements

The views expressed in the article do not necessarily represent the views of the U.S. Department of Energy or the United States Government. Sandia National Laboratories is a multimission laboratory managed and operated by National Technology & Engineering Solutions of Sandia, LLC, a wholly owned subsidiary of Honeywell International Inc., for the U.S. Department of Energy's National Nuclear Security Administration under contract DE-NA0003525.

References

- [1] S. Bograd, P. Reuss, A. Schmidt, L. Gaul, and M. Mayer, "Modeling the dynamics of mechanical joints," *Mechanical Systems and Signal Processing*, vol. 25, no. 8, pp. 2801-2826, 2011.
- [2] L. Gaul and R. Nitsche, "The Role of Friction in Mechanical Joints," *Applied Mechanics Reviews*, vol. 54, no. 2, pp. 93-106, 2001.
- [3] E. P. Petrov and D. J. Ewins, "Analytical Formulation of Friction Interface Elements for Analysis of Nonlinear Multi-Harmonic Vibrations of Bladed Disks," *Journal of Turbomachinery*, vol. 125, no. 2, pp. 364-371, 2003.
- [4] W. Szemplińska-Stupnicka, "The modified single mode method in the investigations of the resonant vibrations of non-linear systems," *Journal of Sound and Vibration*, vol. 63, no. 4, pp. 475-489, 1979.
- [5] M. Krack, L. Panning-von Scheidt, and J. Wallaschek, "A method for nonlinear modal analysis and synthesis: Application to harmonically forced and self-excited mechanical systems," *Journal of Sound and Vibration*, vol. 332, no. 25, pp. 6798-6814, 2013.
- [6] D. Laxalde and F. Thouverez, "Complex non-linear modal analysis for mechanical systems: Application to turbomachinery bladings with friction interfaces," *Journal of Sound and Vibration*, vol. 322, no. 4-5, pp. 1009-1025, 2009.
- [7] H. Festjens, G. Chevallier, and J.-l. Dion, "A numerical tool for the design of assembled structures under dynamic loads," *International Journal of Mechanical Sciences*, vol. 75, pp. 170-177, 2013.
- [8] R. M. Lacayo and M. S. Allen, "Updating structural models containing nonlinear Iwan joints using quasi-static modal analysis," *Mechanical Systems and Signal Processing*, vol. 118, pp. 133-157, 2019.
- [9] E. A. Jewell, M. S. Allen, and R. Lacayo, "Predicting Damping of a Cantilever Beam With a Bolted Joint Using Quasi-Static Modal Analysis," in *ASME 2017 International Design Engineering Technical Conferences and Computers and Information in Engineering Conference*, Cleveland, OH, August 6-9 2017.
- [10] J. H. Ginsberg, *Mechanical and Structural Vibrations: Theory and Applications*, 1st ed., John Wiley and Sons, New York, 2001.
- [11] D. J. Segalman, "A Four-Parameter Iwan Model for Lap-Type Joints," *Journal of Applied Mechanics*, vol. 72, no. 5, pp. 752-760, 2005.
- [12] R. R. J. Craig and M. C. C. Bampton, "Coupling of Substructures for Dynamic Analysis," *AIAA Journal*, vol. 6, no. 7, pp. 1313-1319, 1968.
- [13] W. C. Hurty, "Vibrations of structural systems by component mode synthesis," *Journal of the Engineering Mechanics Division*, vol. 86, no. 4, pp. 51-70, 1960.
- [14] W. C. Hurty, "Dynamic analysis of structural systems using component modes," *AIAA Journal*, vol. 3, no. 4, pp. 678-685, 1965.
- [15] D. A. Najera and R. J. Kuether, "Whole Joint Model Calibration of Discrete Iwan Elements using Quasi-Static Modal Analysis," *Mechanical Systems and Signal Processing (in preparation)*, 2019.
- [16] Cubit Development Team, "CUBIT 15.4 User Documentation," SAND2019-3478 W, Sandia National Laboratories, Albuquerque, NM, 2019.
- [17] R. J. Allemand, "The modal assurance criterion—twenty years of use and abuse," *Sound and vibration*, vol. 37, no. 8, pp. 14-23, 2003.